STRATIGRAPHIC FRAMEWORK AND PETROLEUM GEOCHEMISTRY OLIGOCENE SOURCE ROCKS, NORTHERN SONG HONG BASIN

*Anh Ngoc Le[1], Dat Tien Nguyen[2], Tuan Van Pham[1], Ngan Thi Bui[1],
Hoa Minh Nguyen[1], Muoi Duy Nguyen[1], Hiep Huu Hoang[3]

[1]Hanoi University of Mining and Geology, Vietnam; [2]Vietnam Petroleum Institute, Vietnam; [3]Petrovietnam Exploration Production Corporation (PVEP Song Hong), Vietnam

ABSTRACT: The lacustrine oil-prone organic-rich mudstones in the Oligocene are the most important source rocks which have contributed to generate significant hydrocarbon accumulations in the northern Song Hong basin but still poor understanding due to the limitation of data. Newly c. 800km^2 3D seismic data and well data allows investigating the stratigraphy and geochemistry of the northern Song Hong basin in detail to define the stratigraphic framework and hydrocarbon potential. The area is characterized by three relatively elongate grabens which are separated by the northeast-southwest basement faults. The most completed syn-rift sequence is observed in the central graben and is divided into three distinct sections, lower section (O_l), middle (O_m) and upper (O_u), corresponding to three phases defined by tectonic systems tracts, from rift initiation to rift development and finally fill up phase. Uplift at the end of Oligocene has strongly modified the syn-rift sequences, resulting in folding, reactivated some basement faults and generated a series of new EW trending faults which may act as potential structural traps in the area. Organic geochemical analysis of the lacustrine mudstone samples from O_l and O_m section of well D-1X shows fair to high organic carbon contents, Total Organic Carbon (TOC) 0.51 - 4.86 wt% and Hydrogen Index (HI) 273 - 552 mg HC/g TOC, corresponding to the type II kerogen. Biomarkers indicate the contribution of algal, high land plant, and bacterial sources to the composition of organic matters. Organic matters were deposited in the less oxic environment, in the fresh-water to brackish marine influence.

Keywords: Oligocene source rock, Northern Song Hong basin, lacustrine basin, Rift basin.

1. INTRODUCTION

Paleogene syn-rift successions of many Asian Cenozoic basins are documented from good to excellent source rocks including lacustrine mudstones, coals, and coaly mudstones, which were deposited in lakes, grabens and half grabens [1-5]. Song Hong basin is considered to be a prospective basin, where the dominant source rock is Paleogene lacustrine mudstones [6]. A recent study on a limited number of coal and mudstone samples in Oligocene documented that the mudstones contain 7–17 wt.% Total Organic Carbon (TOC) corresponding mainly to types I and II kerogen. It was deposited in mainly freshwater lakes with oxygen-deficient [4]. Based on the 2D seismic data, the regional occurrence of the lacustrine mudstones in the northeastern part of the Song Hong Basin is predicted by mapping of undrilled Paleogene half grabens [7, 8]. The lack of 3D seismic data and well information affect the accuracy of the results. The newly acquired 3D seismic data of 836 km^2 combined with geochemistry data from a new well allowed a more detailed and consistent breakdown of the geological record into chronostratigraphic events.

This can be used as sequence stratigraphy framework to integrate with petroleum geochemistry for better understanding the linkage of depositional evolution and source rock potential in Paleogene syn-rift successions of the area.

2. GEOLOGICAL SETTING

The study area located offshore, in the northern part of the Song Hong basin which is a Mesozoic – Cenozoic extensional basin. The basin was formed through Paleogene rifting followed by Late Cenozoic thermal sagging [6, 7, 9, 10]. During the rifting stage (from Paleocene to Oligocene), a series of grabens and half-grabens were formed as the result of fault extension and rifting (Fig. 1). They were filled by thick, non-marine Paleogene successions comprising alluvial and lacustrine siliciclastic deposits [11]. End-Oligocene inversion resulted in uplift and truncation of Paleogene strata especially along former Paleogene extensional faults [11]. A distinct unconformity caps the Paleogene syn-rift has been interpreted as a break-up unconformity associated with the incipient opening of the South China Sea [7]. In the post-rift stage (from Miocene to the present time), the study

area lies in the zone affected by various Neogene phases of extension and inversion [7, 12]. Some of the former Paleogene extensional faults were reactivated by modest extension during the Miocene [11]. The basin evolved from the continental non-marine fluvial and lacustrine deposition in the early rifting stage to marine deposition in the late subsiding stage.
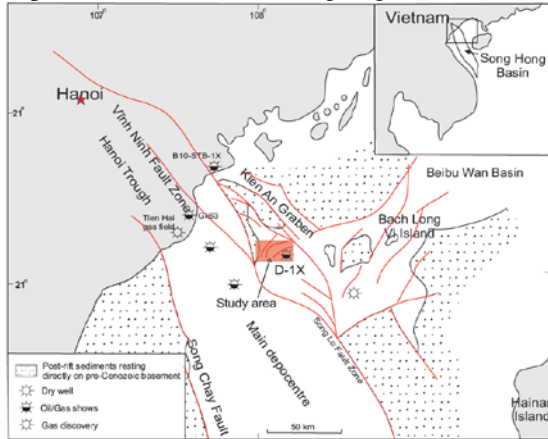
Fig. 1 Location map of the study area in northern Song Hong basin (after [6])

3. DATASET AND METHODOLOGY

The high-quality 3D seismic reflection dataset from offshore Vietnam selected for this study covers an area of 836 km2 with a line spacing of 12.5 m, in the water depth of 25 m - 30 m, 50 km offshore. Standard seismic processing was applied to produce zero-phase seismic data. This study focuses on c. 1 s TWT above the basement, with the dominant frequency of 16 –22 Hz. Well velocity of 1700 m/s is applied for this interval, therefore the seismic resolution is defined as a quarter of the dominant wavelength results in 19 m - 26 m. The interpretation has been carried out using Petrel software with a 125 m × 125 m interpretation grid.

Sixteen mudstone cutting samples of Oligocene age were collected from an exploration well D-1X (Fig. 2) for organic geochemical analysis. The determination of total organic carbon (TOC) was carried out using a Leco CS-200 analyzer. Pyrolysis measurements were performed on the portions (about 50 mg) of pulverized samples using a Rock-Eval 6. A total of eight cuttings were collected from the Oligocene age at different depth for organic extraction. Locations of sampling sites are shown in figure 3.

4. RESULTS

4.1 Paleogene Syn-Rift Deposition

The Paleogene syn-rift sequence is defined by the surface H600 at the base and the H300 on top, on the basis of erosional surfaces and angular unconformities and changing of seismic facies. Seismic to well tie was done to define the surface ages through the well D-1X (Fig. 2).

The Paleogene syn-rift succession is up to 2650 m (2000 ms). There are three relatively elongate grabens, trending northeast-southwest. The Paleogene extensional faults dipping eastward or westward at a high angle of about 600. Each of the graben has dimension as below (Fig. 2):

- East graben: located to the east of the study area; 5 km wide - 17.4 km long - up to 1100 ms deep.
- Central graben: is the largest graben, located at the center of the area; 7.3 km wide - 18.7 km long - up to 1400 ms deep.
- West graben: is a relatively small graben observed in the west of the study area; 8.7 km wide - 6 km long - up to 1400 ms deep.
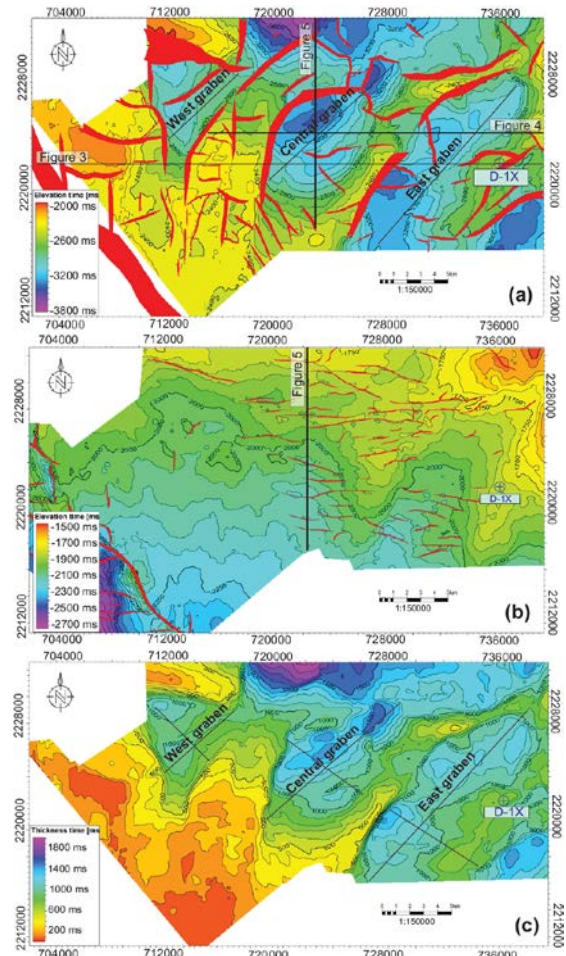
Fig. 2 (a) Time-structure map at the base (H600) and at the top (H300) of the syn-rift sequence (b); the thickness map of the syn-rift sequence is shown in (c) with three elongate graben trending northeast-southwest.

In this paper, to analysis the seismic sequences, the sediment fills in Centre and East graben which have the most completed sequences has been selected to investigate in detail. The deposition begins with a distinct sequence E of low to high amplitude seismic reflections, overlain the basement rock and limit to the top by a very high positive amplitude seismic reflection. This oldest syn-rift deposit is assigned an Eocene age and occurred in the almost entire study area, suggesting for the initial rifting happened during Eocene. It is followed by the Oligocene sequence, which is subdivided into upper (O_u), middle (O_m) and lower (O_l) sections.

The lower section O_l: the section begins with sedimentation located adjacent to steep fault escarpments (average slope of 56^0 and 1370 m high) and extend basinward for 1 – 5 km is chaotic and discontinuous reflections, variable amplitudes, and wedge-shaped geometries (Fig. 3 & 4). Such reflection patterns are indicative of the high-energy sedimentation and interpreted to be the alluvial-fan deposits which are overlaid by well developed lacustrine sequences ranging into system tracts, lowstand-transgressive and highstand system tracts (HST) (Fig. 4). The sequence boundaries can be identified based on the changes in stratal relationships i.e., onlap terminations. Sediment supplied during the development of the system tracts is more closely linked to lake level and is supposed to be a period of hydrologically "balance filled" basin. The initial accommodation rift systems are formed by locally restricted faults, resulting in small, shallow, and disconnected mini-basins rather than a large basin.

The middle section O_m: is characterized by low to high amplitude, wavy and relatively discontinuous seismic reflections due to faulting in Neogene inversion which completely inverts the Paleogene rift. This sub-sequence is widespread and inter-connecting central and east graben form large graben where deep lacustrine facies developed. Sedimentation sources may be from different fault margins of the large graben proving by different directions of downlapping termination (Fig. 4).
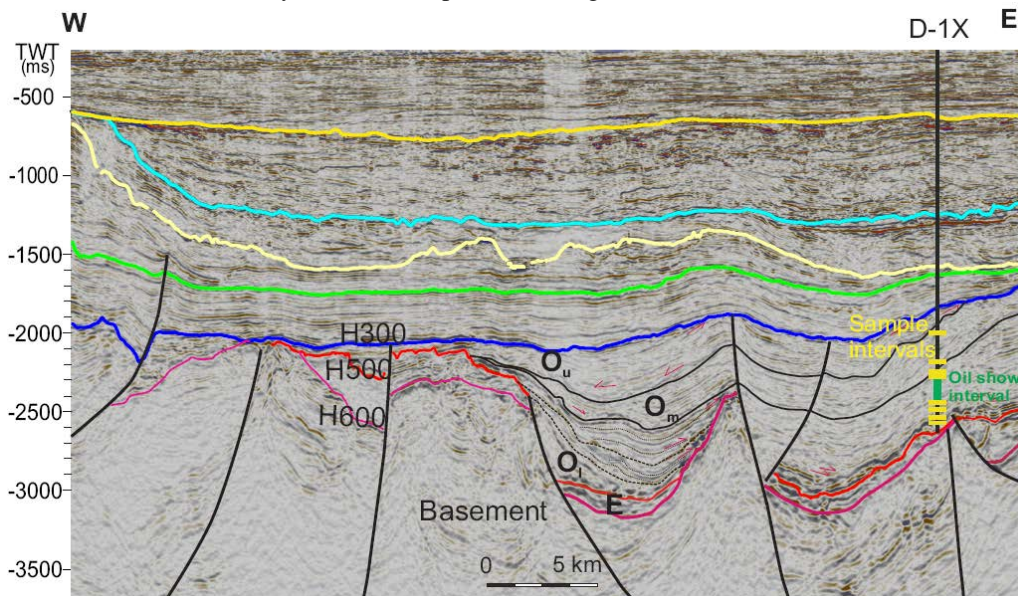
Fig. 3 An East-West seismic section illustrates faults and sequences developed within the grabens (see line location in figure 1). Well penetration in the syn-rift sequence (D-1X) proved for the hydrocarbon occurrence (oil shows) in the O_l section (green color interval). The depth of samples used for petroleum geochemistry analysis has been plotted in yellow

The Upper section O_u: overlaid the O_m and have relatively similar seismic characteristics to the lower section Om. It covers the entire study area and is defined by an unconformity at the base with the downlap termination reflections and is limited to the top by an angular unconformity (H300). This angular unconformity is interpreted as a break-up unconformity associated with the incipient opening of the South China Sea [7]. The

H300 is highly faulted (Fig. 2), with the fault strike EW which are relatively perpendicular to the basement faults with displacements of 10 - 50 ms, and 700 m to 2000 m in length (Fig. 2a), penetrating syn-rift to early post-rift strata. The geographic distribution of faults varies; high areas have almost none, others are cut by many faults (Fig. 2b). Series of E–W-trending faults formed at the end of Oligocene produces a series of potential
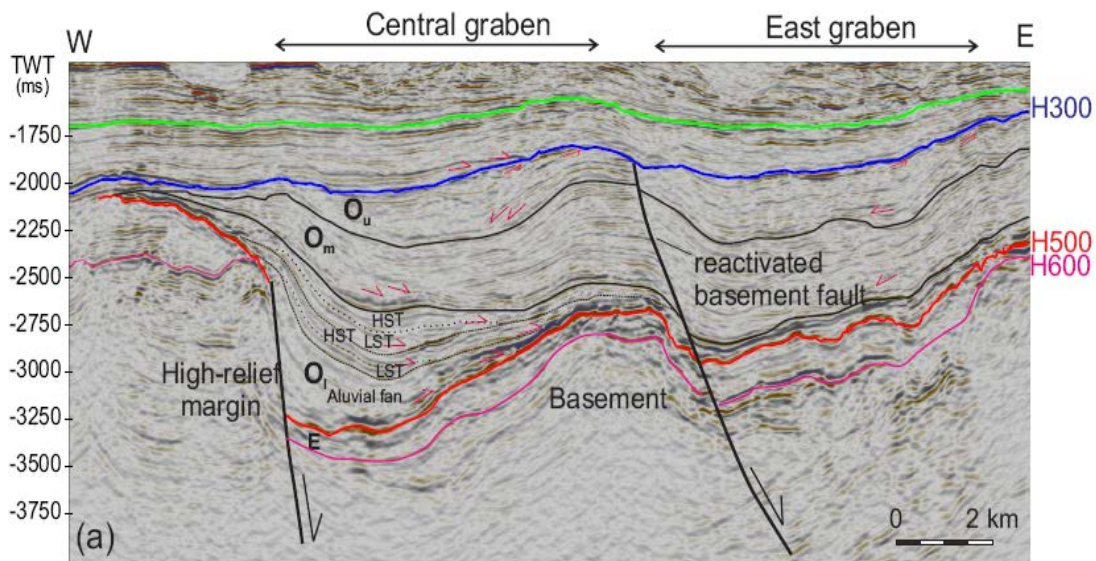
Fig. 4 (a) An interpreted East-West seismic section with three defined tectonic systems tracts. The systems tracts are break-downed into phases in b and c (see the line location in fig. 2).

tilted structural traps.

Rifting in the Song Hong basin is generally considered as Eocene and Oligocene in age [13-15]. However, the Beibuwan Basin reveal rifting commencing already during Early Paleocene time and continuing throughout the Eocene and Oligocene. The relatively constant thickness of sequence O_m in both sides of fault which cut through the Paleogene syn-rift sequences supports for the first interpretation of the two separated rifting phases, one in Eocene and other in Oligocene (Fig. 4). Most of these rift systems were probably inverted and removed during the latest Oligocene-earliest Miocene, resulting in the angular unconformity H300. Fault strike EW is supposed to form in late Oligocene - early Miocene, providing good migration pathways for the syn-rift lacustrine source rocks which are mostly in the gas generation window [6].
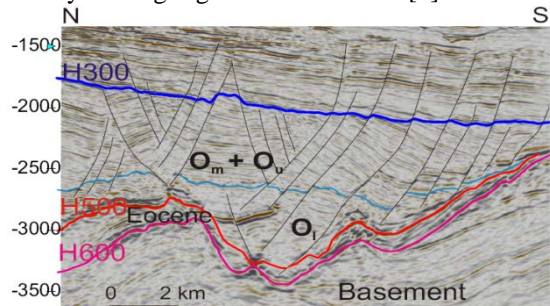
Fig. 5 A north-south seismic section across the central graben showing a series of east-west faults which modified the Oligocene syn-rift sequences
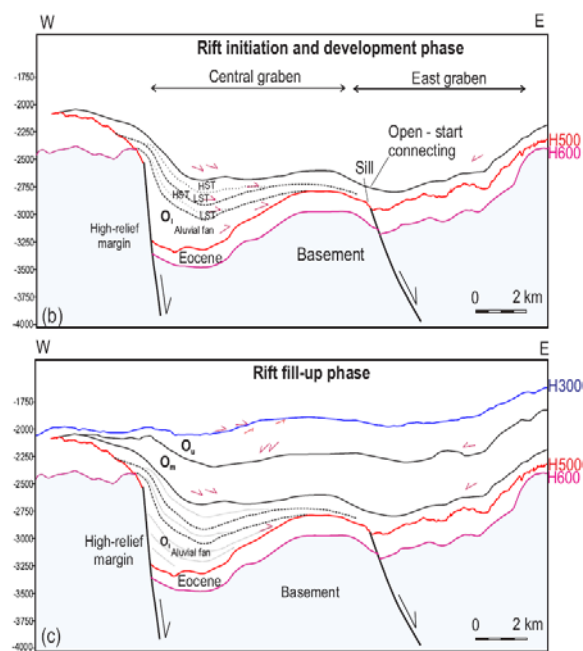
Fig. 4 (b) Line drawing illustrates for the first two phases of rift initiation and rift development results in section O_l, (c) Rift fill-up phase by section O_m and O_u.

4.2. Paleogene Lacustrine Mudstone Source Rock Potential

The study interval comprises of the interlamination of sandstone, siltstone, claystone, calcareous claystone and shale. The uppermost part of Oligocene is characterized by brown claystone, whereas the lower part is presented with grey claystone, black shale.

4.2.1 Bulk geochemical parameters

Bulk geochemical have been analyzed and summarized in Table 1. Depth trends of bulk parameters plotted in Figure 3, corresponding to seismic sections O_1 and O_m. The maximum penetration of the well reaches the base of the O_1 section (Fig. 3). The TOC content is relatively high, mostly above 0.5 wt%. Rock-Eval pyrolytic

(S_1 +S_2) yields of 2.97 - 19.34 mg HC/g Rock, with an average of 6.03 mg HC/g Rock (Table 1, Fig. 6). The HI values range from 273 to 552 mg HC/g TOC (Table 1). A plot of HI vs. Tmax (Fig. 7) reveals that the samples plot along the type II pathways, lie in the field of early maturation.
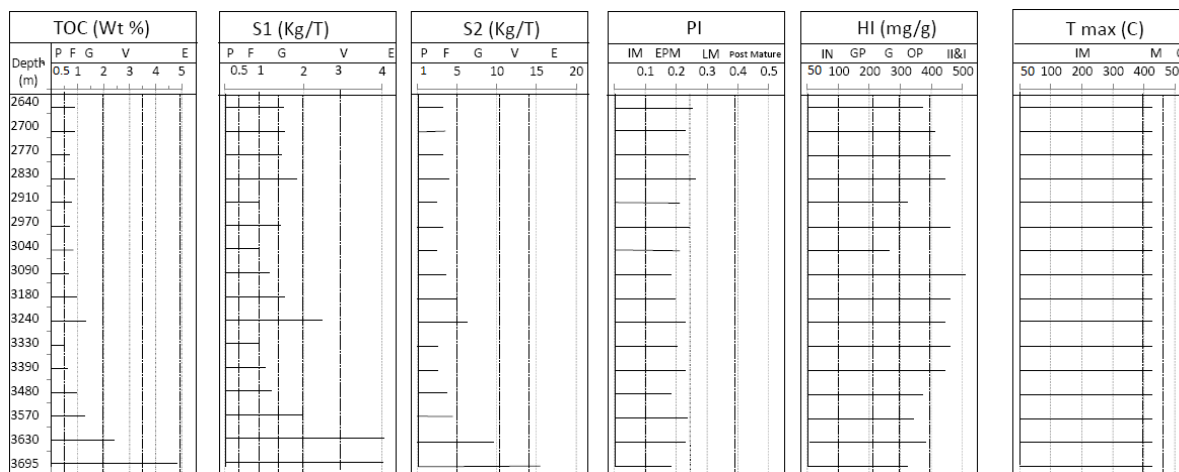
P- Poor; F- Fair; G-good; V- Very good; E- Excellent; Indig- Indigenous Hydrocacbon; Mig- Migrated Hydrocacbon; IM- Immature; EM- Early Mature; M- Mature; LM- Late Mature; IN- Intert Material; GP- Gas Prone; OP – Oil Prone of Kerogen III; O - Oil window.

Fig. 6 Bulk geochemical data from well D-1X (location in Fig. 2)
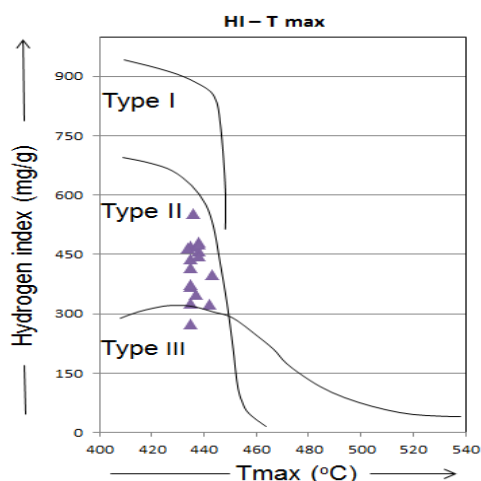
Fig. 7 Hydrogen index (HI) vs. Tmax showing the organic matter type II and early maturity of the studied source rocks, well D-1X

4.2.2 Organic geochemistry (GC-MS)

Soluble organic matter - SOM yields from cutting samples vary between 37 and 159 mg/g TOC (Table 2). The amounts of saturated plus aromatic hydrocarbon contents are around 35 to 62% in the total extract. The saturated hydrocarbon contents are dominant in all extracted samples (between 29 and 43%). Asphaltene contents are

contributed to moderate amounts of around 22 to 30% in SOM yields (table 2). The Pr/Ph ratios range from 1.05 to 1.51, indicating less oxic depositional conditions, likely a lacustrine environment (table 2).

Table 1 Total organic carbon and Rock-Eval

Analysis	Range	Average
TOC (Wt.%)	0.51 - 4.86	1.20
S_1 (mg HC/g Rock)	0.62 – 3.53	1.33
S_2 (mg HC/g Rock)	2.35 – 15.81	4.70
S_1+S_2 (mg HC/g Rock)	2.97 - 19.34	6.03
Tmax (°C)	434 - 443	437
HI (mg HC/g TOC)	273 - 552	414
PI	0.19 – 0.25	0.22

Regular steranes and diasteranes are detected with the variable distribution in the studied samples. The relative abundances of C_{27}, C_{28} and C_{29} sterane are plotted in Fig. 8. Samples contain a high proportion of C_{29} steranes (49 – 72%) which are typically derived from land plants. The predominance of C_{29} steranes also reflects the main contribution of terrestrial organic matter in

the sample. However, the presence of the lower percentage of C_{27} steranes (12 - 34%, table 3) compared to C_{29} steranes indicates the algal origin in the sample. High ratio of C_{30} 4-methylsteranes/C_{29} $\alpha\alpha\alpha R$ steranes, associated with high hydrocarbon source potential, suggest that significant contribution of algae compared to land plant materials in the source rocks. As a result, it is uncertain the extent to which lacustrine or marine environment contributes to the source rock. Organic-rich source rock possibly formed in the large freshwater lake which has delta influence.

The Moretane Index (17β21α hopane/17α21β hopane) is also in the range from immature to early mature source rocks (Table 3). The C_{29} sterane 22S/(22S + 22R) isomer ratios between 0.31 and 0.52 (Table 3), generally below equilibrium of 0.55, whereas the isomeration values of C_{31} hopanes close to the thermal equilibrium value of 0.6, suggesting the source rocks in the early mature window (Rr ~0.6%, Mackenzie, 1984). The MPI-1 values increase downwards, indicating slightly increasing maturity along with the well depth. The calculated vitrinite reflectance values correspond approximately 0.57 – 0.76% (Table 3), generally coinciding with the maturity of source rocks in the early oil window. Organic geochemical analysis indicates that the Oligocene mudstones are a significant potential for oil generation in the Northern Song Hong basin, reaching the early stage of oil generation.
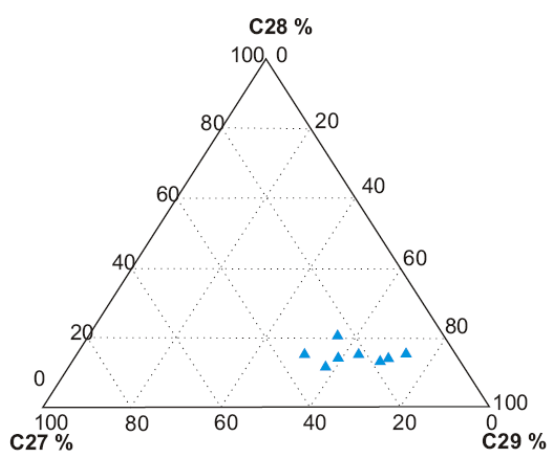
Fig. 8 Triangular plot of regular C_{27}, C_{28}, and C_{29} sterane indicates the dominantly of C_{29} steranes, reflecting the main contribution of terrestrial organic matter in the sample
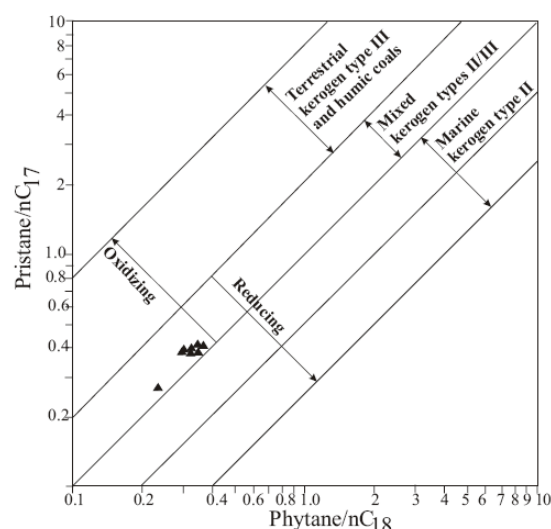
Fig. 9 Pristane/n-C17 versus phytane/n-C18 correlation diagram

Table 2 Soluble organic matter (SOM) yields, relative proportions of saturated and aromatic hydrocarbons, NSO compounds and asphaltenes, the ratio of saturated to aromatic fractions in the SOM yields.

Depth (m)	SOM(mg/gTOC)	Sat. (%)	Aro.(%)	NSO.(%)	Asp.(%)	Sat./ Aro	Pr/ Ph	Pr/ nC$_{17}$	Ph/ nC$_{18}$	CPI-1
2640	54.78	43.80	9.92	24.79	21.49	4.42	1.40	0.39	0.35	1.02
3000	59.29	38.56	9.15	30.07	22.22	4.21	1.51	0.42	0.35	1.59
3070	37.16	39.45	10.09	30.28	20.18	3.91	1.33	0.39	0.36	0.95
3180	81.28	19.86	15.60	29.08	35.46	1.27	1.17	0.33	0.31	1.02
3450	106.61	50.31	12.42	21.74	15.53	4.05	1.62	0.39	0.36	1.01
3540	81.48	27.16	13.36	25.43	34.05	2.03	1.05	0.38	0.35	0.96
3630	159.92	47.55	14.49	24.69	13.27	3.28	1.43	0.27	0.24	1.04
3695	135.80	29.60	15.66	30.60	24.14	1.89	1.46	0.22	0.21	1.00

SOM = soluble organic matter, Sat. = Saturated, Aro. = Aromatic, NSO = Hetero compounds, Asp. = asphaltenes, Pr = pristine, Ph = phytane, CPI = carbon preference index.

Table 3 Concentration ratios of specific biomarkers of studied samples.

Depth (m)	%C$_{27}$ Steranes	% C$_{28}$ Steranes	% C$_{29}$ Steranes	C$_{30}$-4-MSI	C$_{27}$/C$_{29}$ Sterane	Oleanane/ C$_{30}$Hopane	Moretane/ Hopane	20S/(20S+20R) ααα C$_{29}$-Sterane	22S/(22S+22R) C$_{31}$-hopane	MPI-1	Cal. %R$_o$
2640	16.41	15.18	68.41	n.d	0.19	3.03	0.78	0.31	0.60	0.29	0.58
3000	14.40	17.33	68.27	0.21	0.17	4.88	0.54	0.41	0.59	0.28	0.57
3070	24.02	20.89	55.10	0.21	0.30	5.26	0.59	0.40	0.59	0.33	0.60
3180	12.63	14.42	72.95	0.07	0.15	20.01	0.49	0.40	0.60	0.33	0.60
3450	21.00	17.72	61.28	0.33	0.26	17.20	0.21	0.43	0.59	0.43	0.66
3540	32.80	11.76	55.44	0.11	0.37	30.22	0.18	0.34	0.59	0.45	0.67
3630	26.14	14.59	59.27	0.68	0.31	7.48	0.33	0.49	0.59	0.48	0.69
3695	34.10	16.31	49.59	0.40	0.41	15.47	0.47	0.52	0.59	0.60	0.76

C30 4-MPI = ratio of C30 4-methylsteranes to C29 regular steranes, MPI-1 = Methylphenanthrene Index, Cal.%Ro = calculated vitrinite reflectance based on MPI-1.

5. DISCUSSION

5.1. Stratigraphic Evolution

The seismic stratigraphic evolution of the syn-rift sequences is proposed for this study area, along with the concept of [16], to understand the infill of the basin in the relationship between accommodation space and lake level fluctuations vs. sediment input, including three phases defined by tectonic systems tracts.

1. The rift initiation phase occurred at the end of the Eocene, is characterized by isolated and restricted faults which creates early half-grabens, infilled with fluvial fan and deltaic facies under a progradation regime. Sediment sources tend to come from the high-relief basement margin and confined within the central graben which is typed as a shallow lake. Initially, lake level bellows the sill and there is no outflow (Fig. 4b). Outflow from the central graben into the East graben are observed at the end of O$_1$ section. Lake level change can be roughly estimated at about 40m, clearly recorded in the two sequences (Fig. 4b). There is some part of the basin that is not yet a depositional zone which is characterized as sill where the potential accommodation is space below it.

2. The rift development phase. In this phase, there is no clear evidence to see the initial rift faults link and form a larger and deeper depositional area. However, at the end of the sequence O$_1$, the early formed half-grabens tend to be fully filled by O$_1$ sediments and are connected to form a larger deposition area. The formerly nondepositional areas are now subsiding, starting a new period of high accommodation space.

3. Rift fill-up phase by sequences O$_m$, following by O$_u$. The sedimentation regime is progradation and aggradation. Unlike O$_1$ sequence, this filling phase shows the variety of sediment sources, indicated by downlap termination on the base of the O$_m$ and O$_1$ surface. The uplift phase at the end of Oligocene has strongly modified these two sections, resulting in wavy geometry and highly faulted sequences. Faults have an E-W trend and have also documented in the Qiongdongnan basin at the final stage (30–21 Ma) of Paleogene tectonic [15]. In addition, during this time, some early extensional basement faults are reactivated in a reverse sense to formed monoclinal folds which then was a subject of erosion.

5.2 Depositional Environment

The study area has experienced less oxic conditions and marine influence which have good agreement with the sample from immature outcrop samples on the Bach Long Vi Island. However, samples in this study show the higher maturity of organic matters comparing to Bach Long Vi Island outcrop samples which are proved on the plot of pristane/n-C$_{17}$ versus phytane/n-C$_{18}$ (Fig. 9). This more maturation is possibly related to the deeper burial depth of the samples. It, therefore, can be concluded that the Paleogene syn-rift sequences developed from terrestrial (O$_1$) to a mixture between terrestrial and marine sources (O$_m$). From O$_m$ the area continued subsidence, rift fills is possibly more marine influence until the totally open-marine at the end of the rift sequence.

6. CONCLUSIONS

In the study area, the Oligocene syn-rift succession is up to 2650 m and mostly distributed in three grabens, including east graben, centre graben, and west graben, which are separated by northeast-southwest basement faults. The syn-rift sequences have been divided into lower, middle

and upper Oligocene based on the occurrence of unconformities and seismic facies changes. The lower section (O_l) corresponds to rift initiation and rift development phases. Rift initiation created a series of elongate Northeast- southwest grabens with the early sedimentation characterized as organic-rich sediments. It is followed by two identified sequences proved for the lake level fluctuation of about 40 m, corresponding to the rift development phase. Rift fill-up phase includes two sections, O_m and O_u, with the sedimentation regime is progradation and aggradation.

Sediments were deposited in the balance -filled changing to the over-filled rift lake system, in fresh-water to brackish marine influence, less oxic environment. The best source rock intervals are located in the lower part of the well (within O_l section) tied with high amplitude continuous seismic reflectors (TOC: 0.51- 4.96 wt%; high HI up to 552 mg HC/g TOC). The whole syn-rift sequences have experienced uplift phase at the end of Oligocene, creating a series of east-west trending faults, giving great potential for hydrocarbon traps and migration pathways from the matured source rock in the graben centre.

7. REFERENCES

[1] Noble, R., C. Wu, and C. Atkinson, Petroleum generation and migration from Talang Akar coals and shales offshore NW Java, Indonesia. Organic Geochemistry, 1991. 17(3): p. 363-374.

[2] Hasiah, A.W., Oil-generating potential of Tertiary coals and other organic-rich sediments of the Nyalau Formation, onshore Sarawak. J. of Asian Earth Sci., 1999. 17(1-2): p. 255-267.

[3] Curiale, J., Morelos, J., Lambiase, J. and Mueller, W., 2000. Brunei Darussalam: Characteristics of selected petroleums and source rocks. Organic Geochemistry, 31(12), pp.1475-1493.

[4] Petersen, H.I., Andersen, C., Anh, P.H., Bojesen-Koefoed, J.A., Nielsen, L.H., Nytoft, H.P., Rosenberg, P. and Thanh, L., 2001. Petroleum potential of Oligocene lacustrine mudstones and coals at Dong Ho, Vietnam—an outcrop analogue to terrestrial source rocks in the greater Song Hong Basin. Journal of Asian Earth Sciences, 19(1-2), pp.135-154.

[5] Quan, V. and P. Giao, Geochemical evaluation of shale formations in the northern Song Hong basin, Vietnam. Journal of Petroleum Exploration and Production Technology, 2019: p. 1-15.

[6] Andersen, C., Mathiesen, A., Nielsen, L.H., Tiem, P.V., Petersen, H.I. and Dien, P.T., 2005. Distribution of source rocks and maturity modelling in the northern Cenozoic Song Hong Basin (Gulf of Tonkin), Vietnam. Journal of Petroleum Geology, 28(2), pp.167-184.

[7] Rangin, C., Klein, M., Roques, D. and Le Pichón, X., 1995. The Red river fault system in the Tonkin Gulf, Vietnam. Tectonophysics, 243(3-4), pp.209-222.

[8] Andersen, C., Tiem, P.V., Mathiesen, A. and Nielsen, L.H., 1998, May. Some new thermal maturity modelling results using Yükler 1D software and seismic facies mapping in the northern part of the Song Hong Basin. In Conference on Vietnam Petroleum Institute (Vol. 20, pp. 273-284).

[9] Huang, B., Zhu, W., Tian, H., Jin, Q., Xiao, X. and Hu, C., 2017. Characterization of Eocene lacustrine source rocks and their oils in the Beibuwan Basin, offshore South China Sea. AAPG Bulletin, 101(9), pp.1395-1423.

[10] Zhao, Z., Sun, Z., Wang, Z., Sun, Z., Liu, J. and Zhang, C., 2015. The high resolution sedimentary filling in Qiongdongnan Basin, northern South China Sea. Marine Geology, 361, pp.11-24.

[11] Fyhn, M.B., Cuong, T.D., Hoang, B.H., Hovikoski, J., Olivarius, M., Tuan, N.Q., Tung, N.T., Huyen, N.T., Cuong, T.X., Nytoft, H.P. and Abatzis, I., 2018. Linking Paleogene Rifting and Inversion in the Northern Song Hong and Beibuwan Basins, Vietnam, With Left-Lateral Motion on the Ailao Shan-Red River Shear Zone. Tectonics, 37(8), pp.2559-2585.

[12] Fyhn, M.B. and P.V. Phach, Late Neogene structural inversion around the northern Gulf of Tonkin, Vietnam: Effects from right-lateral displacement across the Red River fault zone. Tectonics, 2015. 34(2): p. 290-312.

[13] Clift, P.D. and Z. Sun, The sedimentary and tectonic evolution of the Yinggehai–Song Hong basin and the southern Hainan margin, South China Sea: Implications for Tibetan uplift and monsoon intensification. Journal of Geophysical Research: Solid Earth, 2006. 111(B6).

[14] Zhu, M., S. Graham, and T. McHargue, The red river fault zone in the Yinggehai Basin, South China Sea. Tectonophysics, 2009. 476(3-4): p. 397-417.

[15] Zhang, C., Wang, Z., Sun, Z., Sun, Z., Liu, J. and Wang, Z., 2013. Structural differences between the western and eastern Qiongdongnan Basin: evidence of Indochina block extrusion and South China Sea seafloor spreading. Marine Geophysical Research, 34(3-4), pp.309-323.

[16] Holz, M., Vilas-Boas, D.B., Troccoli, E.B., Santana, V.C. and Vidigal-Souza, P.A., 2017. Conceptual models for sequence stratigraphy of continental rift successions. In Stratigraphy & Timescales (Vol. 2, pp. 119-186). Academic Press.